Supporting information for:

Insight on shallow trap states introduced photocathodic performance in n-type polymer photocatalysts

Qiushi Ruan,[a,1] Tina Miao,[a,b,1] Hui Wang,[a] Junwang Tang*[a]

[1] Both authors contributed equally

[a] Department of Chemical Engineering, University College London (UCL), WC1E 7JE, London, United Kingdom

[b] Department of Chemistry, University College London (UCL), WC1H 0AJ, London, United Kingdom

XRD patterns were collected by a D8 Bruker Diffractometer. The UV-Vis absorption spectra were collected using a Shimadzu UV-Vis 2550 spectrophotometer fitted with an integrating sphere using $BaSO_4$ as the reference material. XPS measurements were done on a Thermoscientific XPS K-alpha surface analysis machine using an Al source. Analysis was performed on the Casa XPS software. SEM images were taken by a JEOL JSM-7401F Scanning Electron Microscope. BET measurements were performed by a Tri Star II. NMR spectra were performed with a solid state NMR spectrometer, Ascend™, 300WB, Bruker. PL spectra were collected by a Renishaw InVia Raman Microscope (325nm).

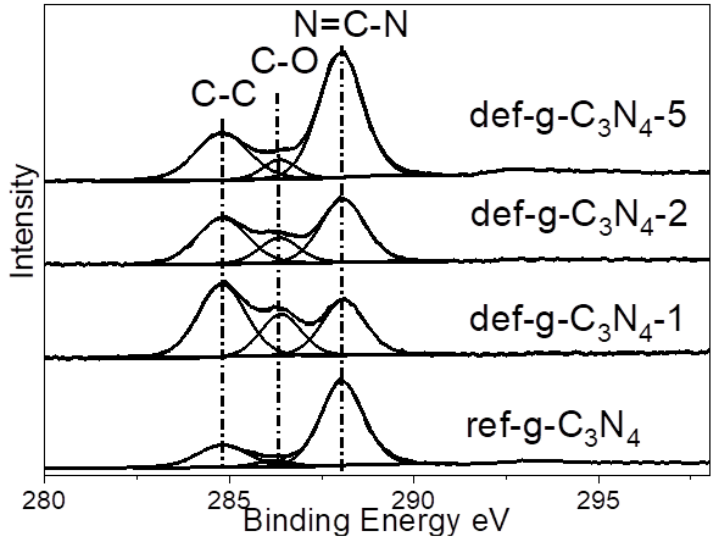

Figure S1. XPS C1s spectra of all samples

Table S1. The ratio of C-O bond to N=C-N bond and C to N ratio in all samples

Sample	Ratio of C-O/N=C-C	C_xN_y
ref-g-C_3N_4	0.047±0.007	$C_3N_{4.10\pm0.03}$
def-g-C_3N_4-1	0.58±0.16	$C_3N_{3.18\pm0.12}$
def-g-C_3N_4-2	0.33±0.07	$C_3N_{3.65\pm0.04}$
def-g-C_3N_4-5	0.13±0.01	$C_3N_{3.61\pm0.01}$

Table S2 Surface area of def-g-C_3N_4-1, def-g-C_3N_4-2 and def-g-C_3N_4-5 samples determined by BET measurements.

	Surface area (m^2/g)
g-C_3N_4	10.9
def-g-C_3N_4-1	12.9
def-g-C_3N_4-2	13.4
def-g-C_3N_4-5	18.5

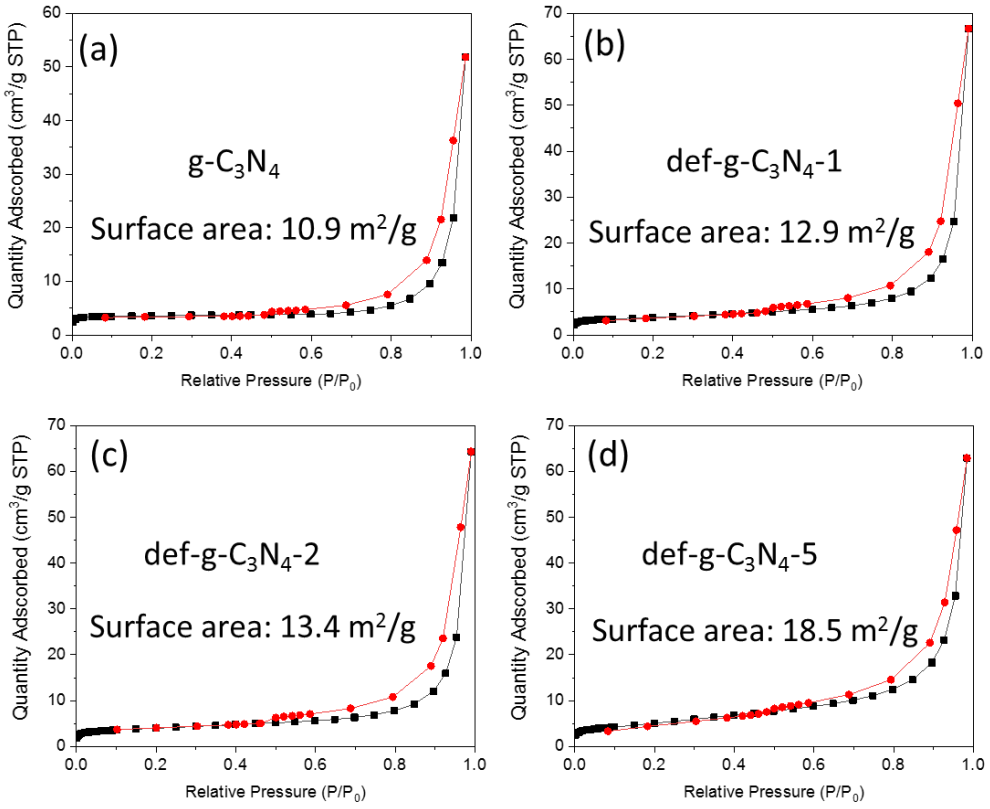

Figure S2 BET measurement of g-C_3N_4, def-g-C_3N_4-1, def-g-C_3N_4-2 and def-g-C_3N_4-5 samples

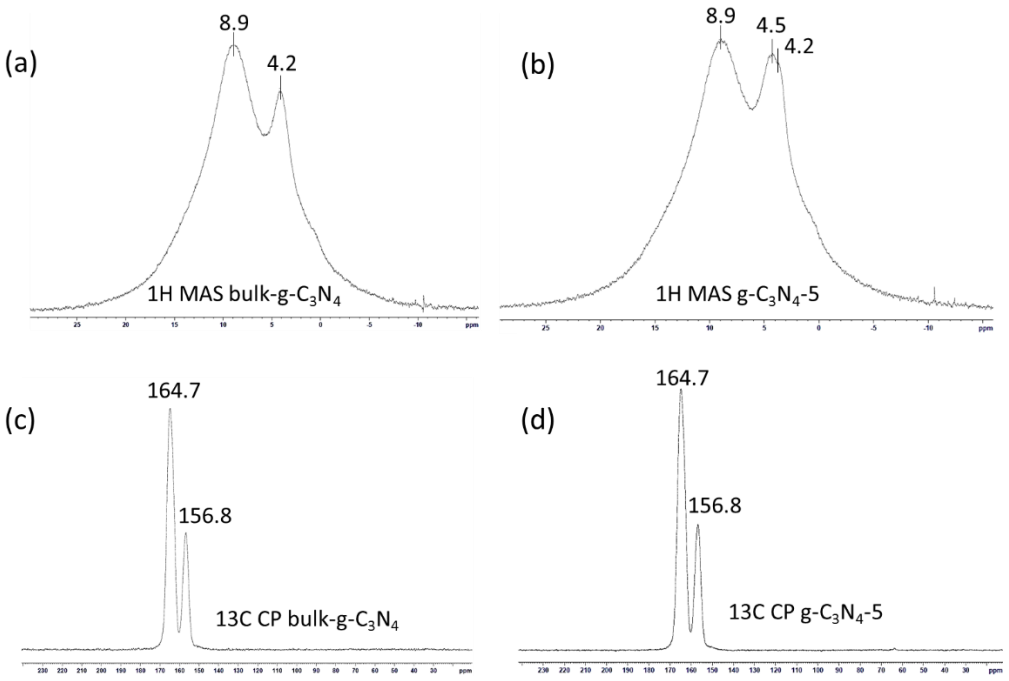

Figure S3. ^{1}H MAS solid state NMR spectra of (a) reference bulk-g-C_3N_4 and (b) def-g-C_3N_4-5, as well as ^{13}C CP MAS solid state NMR spectra of (c) reference bulk-g-C_3N_4 and (d) def-g-C_3N_4-5.

^{1}H Solid state NMR spectrum of ref-g-C_3N_4 contains two main peaks at 8.9 ppm and 4.2 ppm, which can be attributed to the chemical shifts of –NH_x ending group and residual water, respectively.[1] An additional clear peak locating at 4.5 ppm is present in def-g-C_3N_4-5 sample and can be ascribed to the formation C-OH bonds.[1] ^{13}C solid state NMR spectra of these two samples show two similar peaks at 156.8 ppm and 164.7 ppm, which has been assigned to C-$[N]_3$ and $CN_2(NH_2)$ groups, respectively[2]

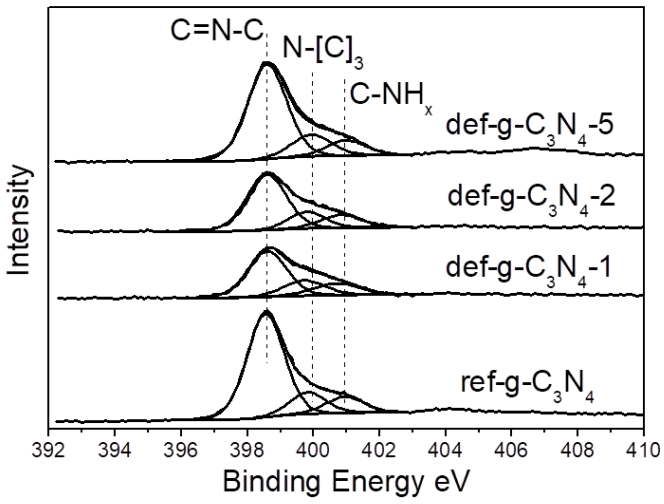

Figure S4 XPS N1s spectra of all g-C_3N_4 samples

Table S3 Percentage breakdown of different bonds and ratios of bonds within the N1s spectra

	C=N-C (sp^2)	N-[C]$_3$ (sp^3)	C-NH$_x$	sp^2 to sum of sp^3 and C-NH$_x$
Binding Energy (eV)	398.7	399.9	401.0	
ref-g-C_3N_4	74.2%	15.7%	10.2%	2.9
def-g-C_3N_4-1	63.8%	20.9%	15.3%	1.8
def-g-C_3N_4-2	66.3%	18.2%	15.5%	2.0
def-g-C_3N_4-5	72.0%	16.5%	11.5%	2.6

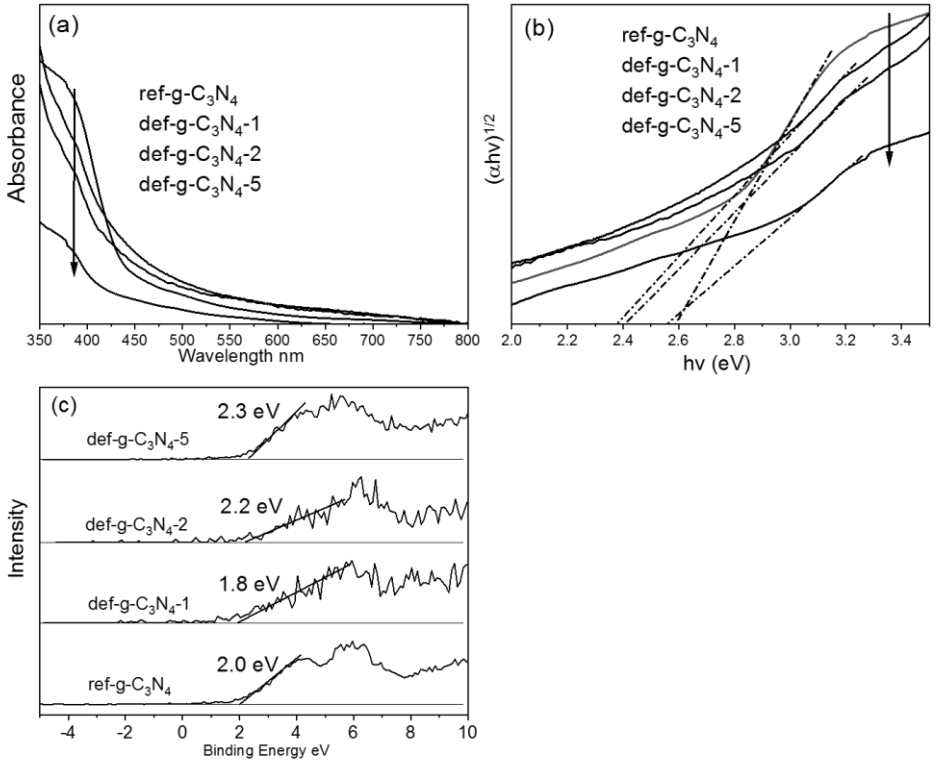

Figure S5. (a) UV-vis spectra, (b) Tauc plots and (c) XPS valence band spectra of ref-g-C_3N_4, def-g-C_3N_4-1, def-g-C_3N_4-2 and def-g-C_3N_4-5 films

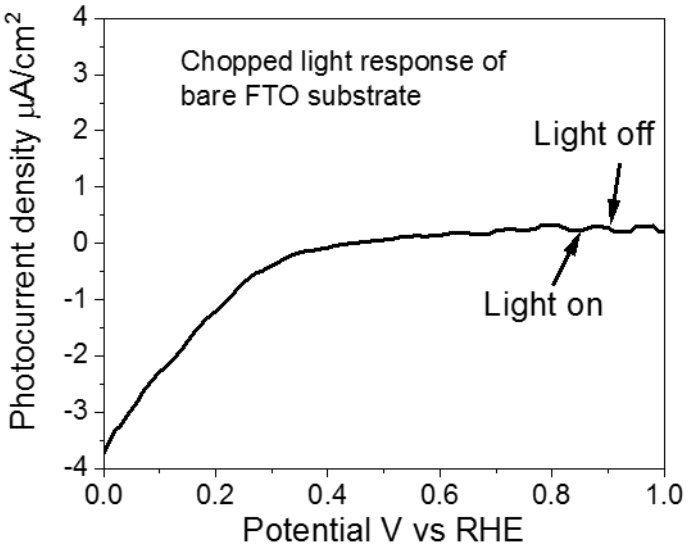

Figure S6 Chopped light-response of bare FTO substrate.

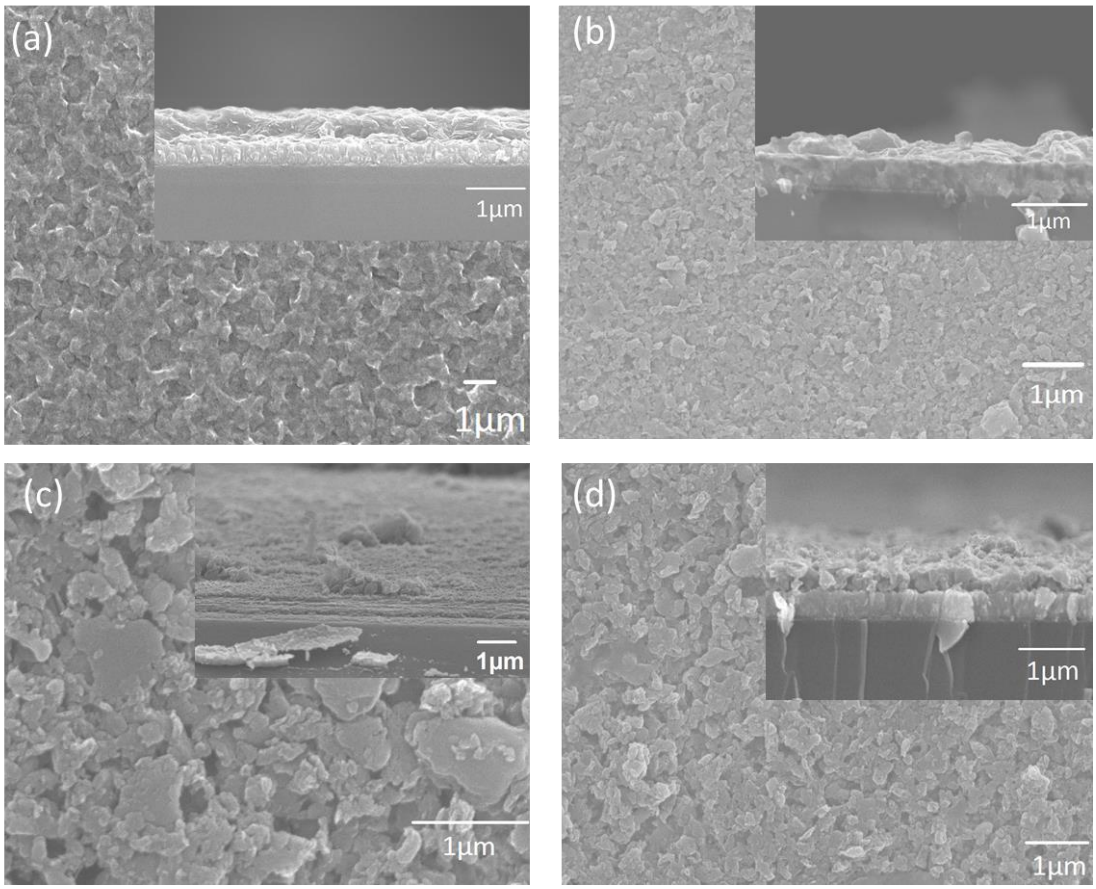

Figure S7. SEM images of (a) ref-g-C_3N_4, (b) def-g-C_3N_4-1, (c) def-g-C_3N_4-2 and (d) def-g-C_3N_4-5 films

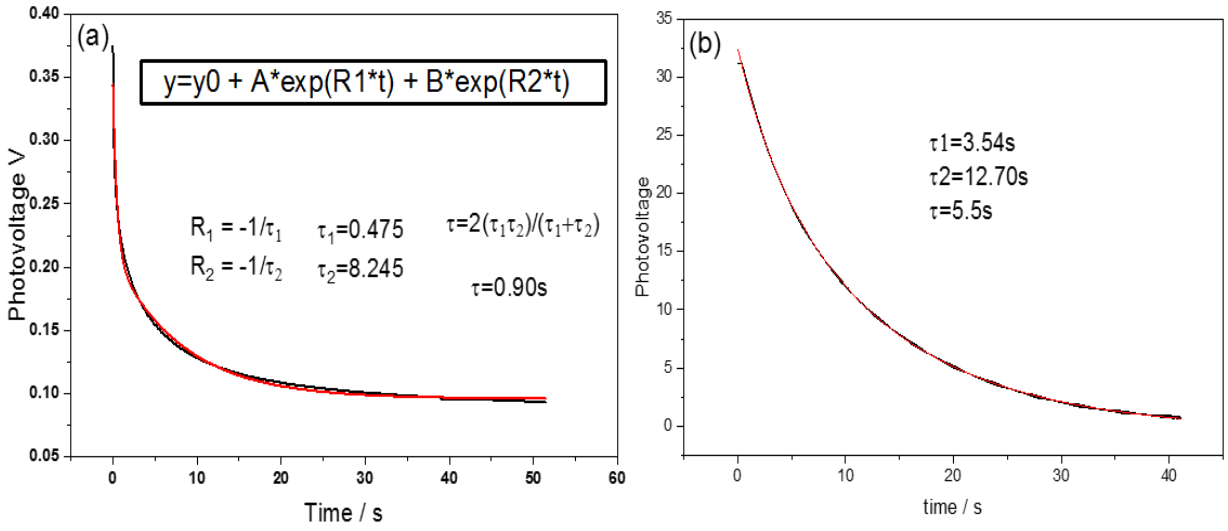

Figure S8. determination of average electron lifetime of (a) ref-g-C_3N_4 and (b) def-g-C_3N_4-5 films

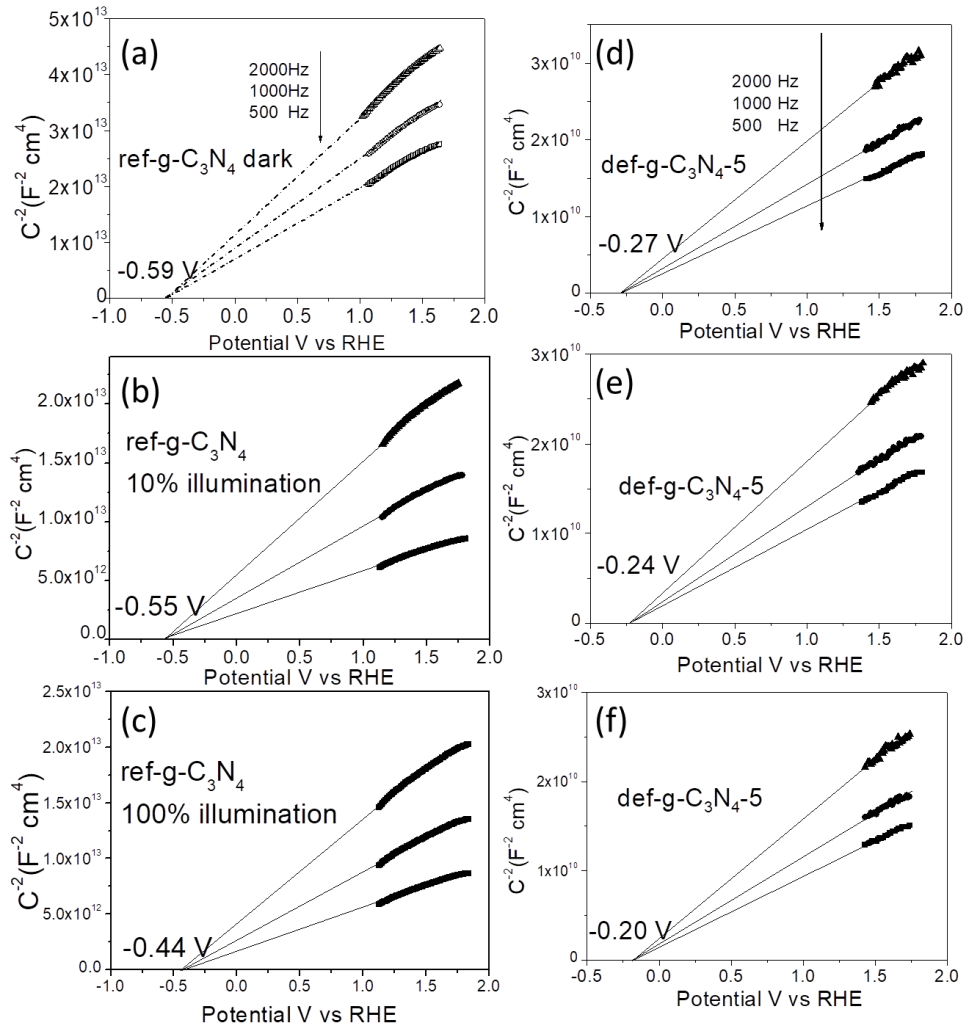

Figure S9 (a-c) Mott-schottky plots of ref-g-C_3N_4 electrode at 500 Hz, 1000 Hz and 2000 Hz with 0% - 100% illumination; (d-f) Mott-schottky plots of def-g-C_3N_4-5 electrode at 1 KHz with 0% - 100% illumination;

Table S4 Carrier density N_D and depletion layer width of ref-g-C_3N_4 and def-g-C_3N_4-5 samples

	Measured slope (1000 Hz)	N_D (ε_r=7.7)	W_{sc} (ε_r=7.7; 0V vs RHE)
ref-g-C_3N_4 dark	$1.57*10^{13}$	$1.2*10^{18}$ (cm^{-3})	22 nm
10% illumination	$6.18*10^{12}$	$3.1*10^{18}$ (cm^{-3})	/
100% illumination	$6.13*10^{12}$	$3.1*10^{18}$ (cm^{-3})	/
def-g-C_3N_4-5	$1.10*10^{10}$	$1.7*10^{21}$ (cm^{-3})	0.4 nm
10% illumination	$1.03*10^{10}$	$1.8*10^{21}$ (cm^{-3})	/
100% illumination	$0.98*10^{10}$	$1.9*10^{21}$ (cm^{-3})	/

$$\frac{1}{C^2} = \frac{2}{\varepsilon\varepsilon_0 A^2 e N_D}(V - V_{fb} - \frac{k_B T}{e})$$

$$slope = \frac{2}{\varepsilon\varepsilon_0 A^2 e N_D}$$

$$W_{sc} = \sqrt{\frac{2\varepsilon_0\varepsilon_r}{eN_D}(V - V_{fb} - \frac{k_B T}{e})}$$

ε_0 is the vacuum permittivity: $8.854187817\times10^{-14}$ F/cm, ε_r is the static dielectric constant: it is 7.7 for c-C_3N_4[3] and current not available for g-C_3N_4; A is the area: 1 cm^2; e is the electron charge: 1.6×10^{-19}C.

Table S5. Analysis of impedance plots of ref-g-C_3N_4 and def-g-C_3N_4-5; R_s is the system resistance, R_{ct} is the charge transfer resistance, CPE is the constant phase element representing the double layer capacitor.

	R_s (Ω cm^2)	R_{ct} / (Ω cm^2)	CPE (S^n Ω^{-1} cm^{-2})	N
ref-g-C_3N_4	218 (±116.93%)	$1.3 * 10^5$ (±0.46%)	$8.1 * 10^{-7}$ (±1.26%)	0.94 (±0.49%)
def-g-C_3N_4-5	49 (±27.35%)	$5.6 * 10^3$ (±0.86%)	$4.5 * 10^{-5}$ (±1.71%)	0.85 (±0.90%)

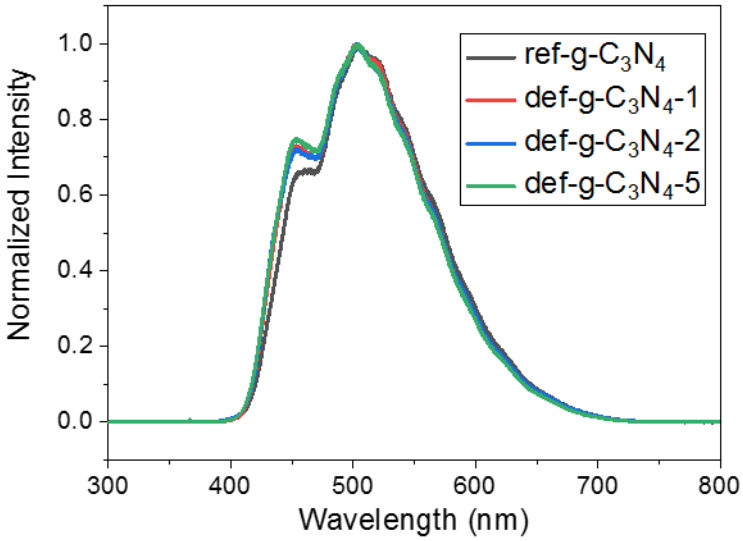

Figure S10. Normalised photoluminescence spectra of ref-g-C_3N_4, def-g-C_3N_4-1, def-g-C_3N_4-2 and def-g-C_3N_4-5 samples after 325 nm excitation, recorded using a Renishaw InVia Raman Microscope (325nm)

Photoluminescence (PL) spectroscopy was undertaken using a 325 nm laser probe. The PL signal peaks around 450 and 500 nm are assigned to the π–π* transitions and n–π* emission, respectively.[4]

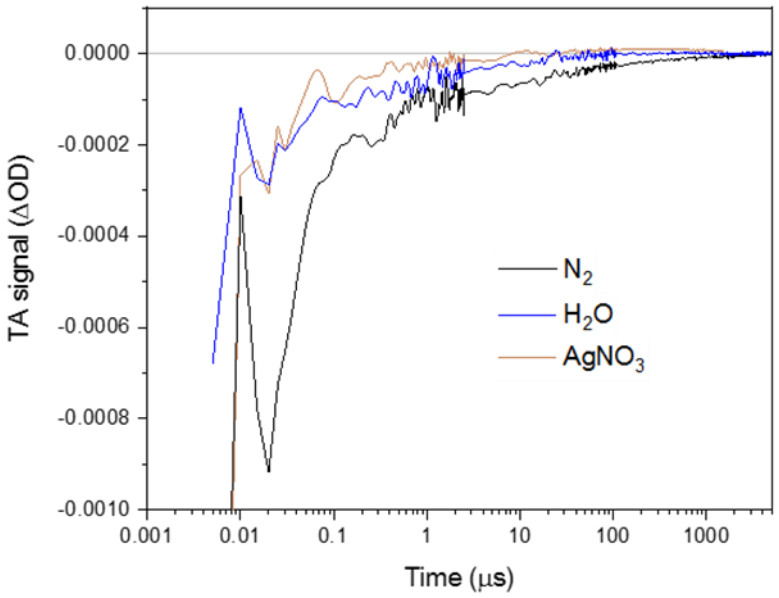

Figure S11 TAS spectra of def-g-C_3N_4-1 sample in N_2, (N_2-flushed) water and (N_2-flushed) 2mM $AgNO_3$ solution.

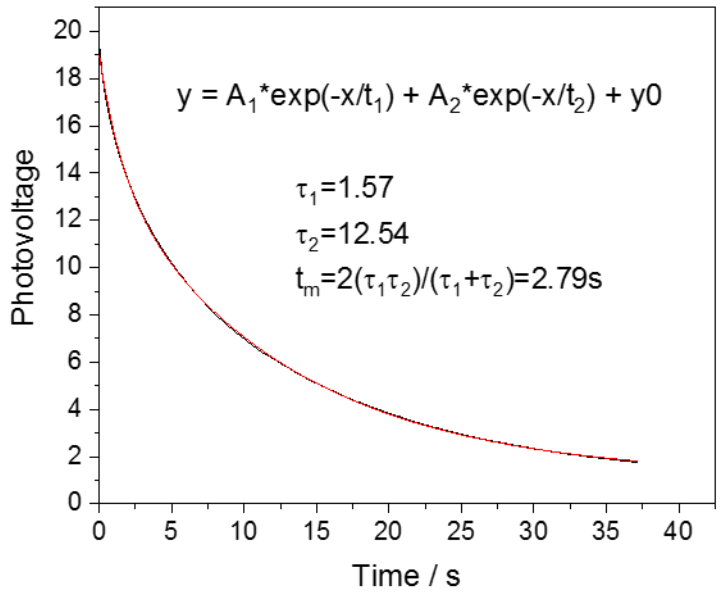

Figure S12. OCVD curve (black) and fitted analysis (red) of H_2O_2 treated ref-g-C_3N_4 sample

Reference

1. Zhang, Q.; Chen, P.; Tan, C.; Chen, T.; Zhuo, M.; Xie, Z.; Wang, F.; Liu, H.; Cai, Z.; Liu, G., A photocatalytic degradation strategy of PPCPs by a heptazine-based CN organic polymer (OCN) under visible light. *Environmental Science: Nano* **2018,** *5* (10), 2325-2336.

2. Wang, Y.; Bayazit, M. K.; Moniz, S. J.; Ruan, Q.; Lau, C. C.; Martsinovich, N.; Tang, J., Linker-controlled polymeric photocatalyst for highly efficient hydrogen evolution from water. *Energy & Environmental Science* **2017,** *10* (7), 1643-1651.

3. Mo, S.-D.; Ouyang, L.; Ching, W.; Tanaka, I.; Koyama, Y.; Riedel, R., Interesting physical properties of the new spinel phase of Si 3 N 4 and C 3 N 4. *Physical Review Letters* **1999,** *83* (24), 5046.

4. Jorge, A. B.; Martin, D. J.; Dhanoa, M. T.; Rahman, A. S.; Makwana, N.; Tang, J.; Sella, A.; Corà, F.; Firth, S.; Darr, J. A., H2 and O2 evolution from water half-splitting reactions by graphitic carbon nitride materials. *The Journal of Physical Chemistry C* **2013,** *117* (14), 7178-7185.